Wind Structure and Wind Loading

Brorsen, Michael

Publication date:
2007

Document Version
Publisher's PDF, also known as Version of record

Wind Structure and Wind Loading

Michael Brorsen

ISSN 1901-7286
DCE Lecture Notes No. 12

Department of Civil Engineering

Aalborg University
Department of Civil Engineering
Section of Water and Soil

DCE Lecture Notes No. 12

Wind Structure and Wind Loading

by

Michael Brorsen

March 2007

Scientific Publications at the Department of Civil Engineering

Technical Reports are published for timely dissemination of research results and scientific work carried out at the Department of Civil Engineering (DCE) at Aalborg University. This medium allows publication of more detailed explanations and results than typically allowed in scientific journals.

Technical Memoranda are produced to enable the preliminary dissemination of scientific work by the personnel of the DCE where such release is deemed to be appropriate. Documents of this kind may be incomplete or temporary versions of papers-or part of continuing work. This should be kept in mind when references are given to publications of this kind.

Contract Reports are produced to report scientific work carried out under contract. Publications of this kind contain confidential matter and are reserved for the sponsors and the DCE. Therefore, Contract Reports are generally not available for public circulation.

Lecture Notes contain material produced by the lecturers at the DCE for educational purposes. This may be scientific notes, lecture books, example problems or manuals for laboratory work, or computer programs developed at the DCE.

Theses are monograms or collections of papers published to report the scientific work carried out at the DCE to obtain a degree as either PhD or Doctor of Technology. The thesis is publicly available after the defence of the degree.

Latest News is published to enable rapid communication of information about scientific work carried out at the DCE. This includes the status of research projects, developments in the laboratories, information about collaborative work and recent research results.

Published 2007 by
Aalborg University
Department of Civil Engineering
Sohngaardsholmsvej 57,
DK-9000 Aalborg, Denmark

Printed in Denmark at Aalborg University

ISSN 1901-7286 DCE Lecture Notes No. 12

Contents

Chapter 1

Wind structure

1.1 Introduction

The purpose of this note is to provide a short description of wind, i.e. of the flow in the atmosphere of the Earth and the loading caused by wind on structures. The description comprises

- causes to the generation of wind
- the interaction between wind and the surface of the Earth
- the stochastic nature of wind
- the interaction between wind and structures, where it is shown that wind loading depends strongly on this interaction.

1.2 The cause to generation of wind

To describe the details of the weather, including wind, on this planet is a tough job. However, it is possible to get some basic knowledge by doing a few, simple considerations.

The driving force in the generation of wind is the non-uniform solar heating of the Earth' surface. The incident solar radiation per m^2 is simply higher at Equator than at the poles. See Figure 1.1.

If the Earth did not rotate, the heating at Equator would create a buoyancy causing an air mass to ascend. Due to the equation of continuity this flow would cause another flow from the poles towards Equator, and the resulting flow would be as sketched in figure 1.2.

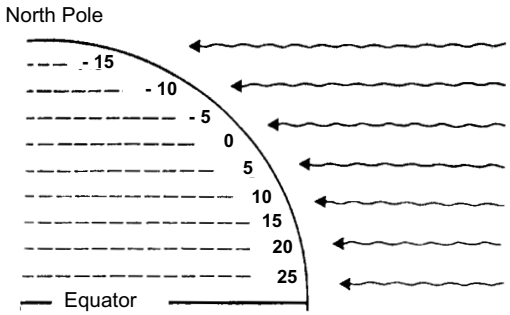

Figure 1.1: Incident solar radiation and temperatures at Equinox

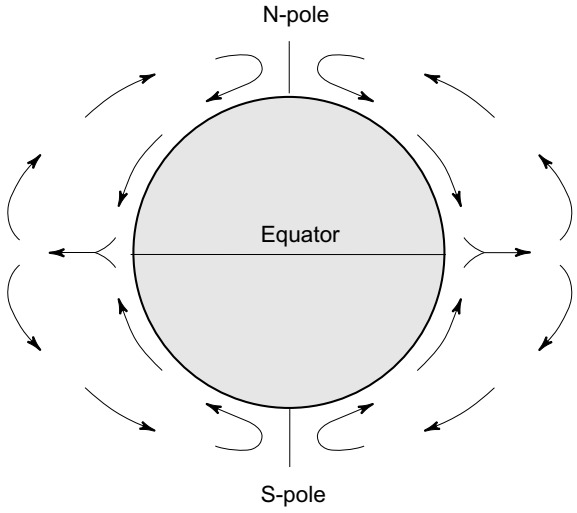

Figure 1.2: Flow in the atmosphere of a non-rotating Earth

In practice this flow do not appear because the Earth actually is rotating. Normally we describe motion in a coordinate system fixed to the Earth, i.e. it is rotating. Seen from this coordinate system, the path of a particle is deflected to the right, when looking in the direction of motion (on the northern hemisphere).

In order to describe this deflection by an ordinary application of Newton's 2nd law, it is necessary to include the fictive *Coriolis' force*. However, if we had described the motion in an inertial system, i.e. a non-rotating system fixed to the universe, this fictive force would not be necessary.

Seen from a system fixed to the Earth the wind at a large height would blow to the north after the ascent, but it is deflected to the east due to Coriolis' force. After some time the air is also cooled so much that it will descent due to a negative buoyancy. In this way the most southern flow cell is formed, see Figure 1.3.

As cold air flows from the north pole in southerly direction close to the ground, one might expect the formation of only one more flow cell. However, this is not possible,

because formation of only two cells would yield simultaneous flow in two directions, where the two cells would meet. Instead a third flow cell is formed, which makes the flows interact correctly, see Figure 1.3.

In a similar way 3 flow cells are formed on the southern hemisphere, but there the Coriolis' force is acting to the left.

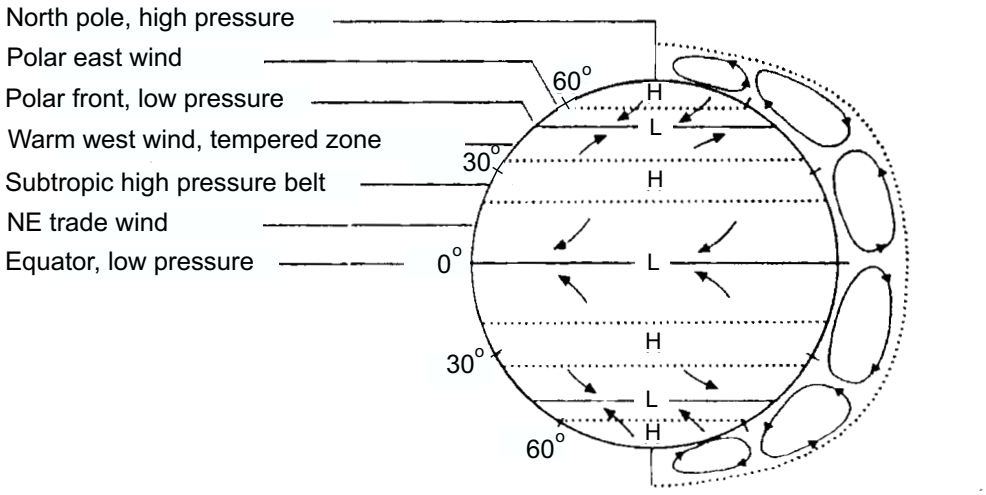

Figure 1.3: Sketch of the flow cell pattern in the atmosphere. The scale in radial direction is strongly exaggerated. In reality the flow takes place under 10-15 km's height corresponding to less than 1/10 mm in the sketch.

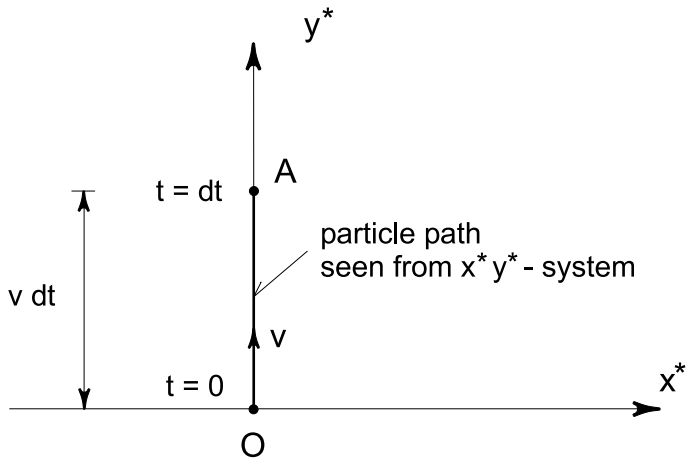

Figure 1.4: Motion described in the fixed $x^*\,y^*$-system

1.3 Coriolis' force

Coriolis' force is the fictive external force, which it is necessary to include in Newton's 2nd law on order to describe the motions correctly in a rotating coordinate system. The reason why Coriolis' force has to be introduced is shown below.

A particle is assumed to move at constant velocity $\vec{v}$ along a straight particle path in the $x^*\,y^*$-system, which is fixed to the universe. According to Newton's 2nd law no external forces are acting on this particle.

The particle is at point O at time $t = 0$, and it is moving along the y^*-axis. At time $t = 0 + dt$ it has moved the distance $v\,dt$ up to point A. See Figure 1.4.

The same motion is now described in the $x\,y$-system, rotating at angular velocity $\vec{\omega}$. Seen from the $x\,y$-system, the $x^*\,y^*$-system has been turned the angle $\omega\,dt$ *clock wise* during the dt seconds, and in this period the particle has moved from point O to point A.

Seen from the rotating system the particle is moving along the y-axis at $t = 0$, but the particle path is deflected to the right in such a way that the particle ends up at point A at the time dt. The path is thus curved even though no external forces has acted on the particle. See Figure 1.5.

If we want to apply Newton's 2nd law to describe the motion in the rotating system, we have to introduce the fictive Coriolis' force acting to the right, when looking in the direction of the motion.

In e.g. Meriam and Kraige (1987) the Coriolis' force, here denoted $\vec{F}_C$, reads:

$$\vec{F}_C = -2\,m\,\vec{\omega} \times \vec{v} \tag{1.1}$$

where m is the mass of the particle.

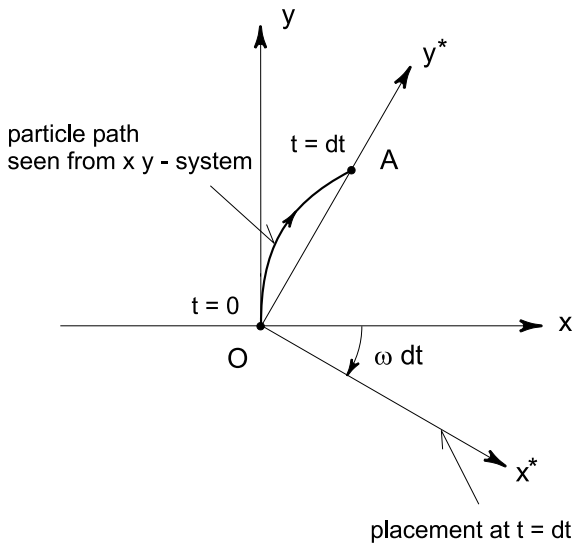

Figure 1.5: Motion described in the rotating $x\,y$-system

At latitude λ, it is natural to describe the motion in a rotating coordinate system, where the $x\,y$-plane is the tangent plane to the ground and the x-axis is parallel to the latitude, see Figure 1.6.

In the $x\,y$-system the expressions for the angular velocity of the Earth, $\vec{\omega}$, and the velocity of the particle,$\vec{v}$, reads:

$$\vec{\omega} = (\omega_x, \omega_y, \omega_z) = (0, \omega\,\cos\lambda, \omega\,\sin\lambda) \tag{1.2}$$

and

$$\vec{v} = (v_x, v_y, v_z) \tag{1.3}$$

If the motion is horizontal, $v_z = 0$, one finds:

$$\begin{aligned} \vec{\omega}\ \times\ \vec{v}\ &= \begin{vmatrix} \vec{e}_x & \vec{e}_y & \vec{e}_z \\ 0 & \omega\,\cos\lambda & \omega\,\sin\lambda \\ v_x & v_y & 0 \end{vmatrix} \\ &= (-v_y\,\omega\,\sin\lambda\ , v_x\,\omega\,\sin\lambda\ , -v_x\,\omega\,\cos\lambda) \end{aligned} \tag{1.4}$$

The horizontal component of Coriolis' force on the particle reads:

$$\vec{F}_{C,h} = -2\,m\,\omega\,\sin\lambda\,(-v_y, v_x) = m\,2\,\omega\,\sin\lambda\,\hat{v} \tag{1.5}$$

where $\hat{v}$ is $\vec{v}$ rotated 90° clockwise. Substitution of the so called *Coriolis' parameter*:

$$\boxed{f_C = 2\,\omega\,\sin\lambda} \tag{1.6}$$

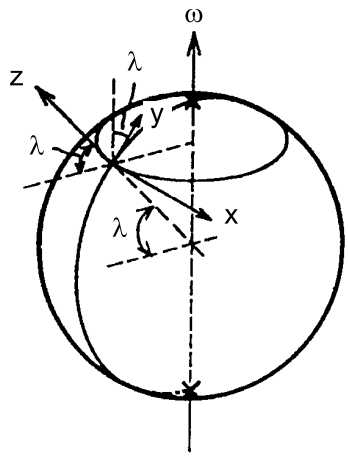

Figure 1.6: Placement of the rotating coordinate system

yields:

$$\boxed{\vec{F}_{C,h} = m\, f_C\, \hat{v} = m\, f_C\, (v_y, -v_x)} \tag{1.7}$$

The size of the horizontal Coriolis' force reads:

$$F_{C,h} = m\, f_c\, v$$

The value of the Coriolis' parameter is small everywhere, and e.g. in Denmark at latitude $\lambda = 56^\circ$ the size of f_C is:

$$f_C = 2\,(2\pi)/(24 \cdot 3600)\, \sin 56^\circ \; = 1.21 \cdot 10^{-4} \;\; \text{rad/sek}$$

In the following it is shown that the Coriolis' force is very important in the description of flow in the atmosphere, even though it is a very small force.

1.4 Weather maps

The pressure at a point is actually the weight of the mass of the air column above the point. Today the unit for pressure is named *hektoPascal* (hPa), where 1 hPa = 100 Pa = 100 N/m^2. This unit is the same as *millibar* (mbar), because 1 millibar = 10^{-3} bar = $10^{-3} \cdot 10^5$ Pa = 100 Pa = 1 hPa. The unit *atmosphere* (atm) is also seen, where 1 atm = 1013 hPa = $1.013 \cdot 10^5$ Pa.

If the atmospheric pressure is measured at a large number of points at the ground, it is possible to draw curves through points with the same pressure. These curves are named *isobars*.

The isobars are closed curves situated around areas with either high or low pressure.

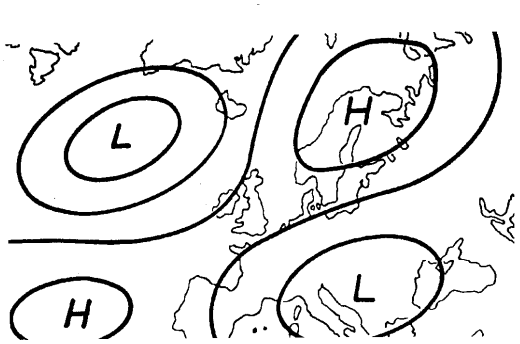

Figure 1.7: Weather map with isobars

A typical course of isobars at winter time is sketched in Figure 1.7. By intuition we expect a flow (wind) that tries to reduce these differences in pressure, i.e. flow from high pressure towards low pressure. See Figure 1.8.

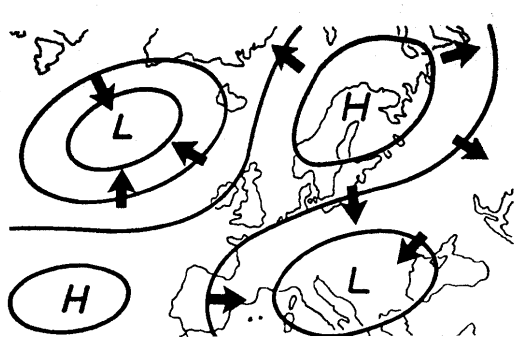

Figure 1.8: Expected directions of wind

This is also attempted by nature, but the Coriolis' force deflects the wind to the right on the northern hemisphere. In practice the deflection is so large that the wind direction is nearly parallel with the isobars. See Figure 1.9.

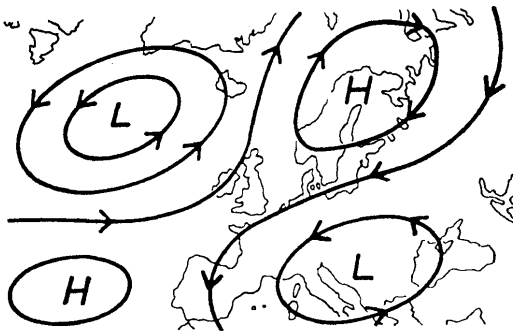

Figure 1.9: Sketch of actual wind directions

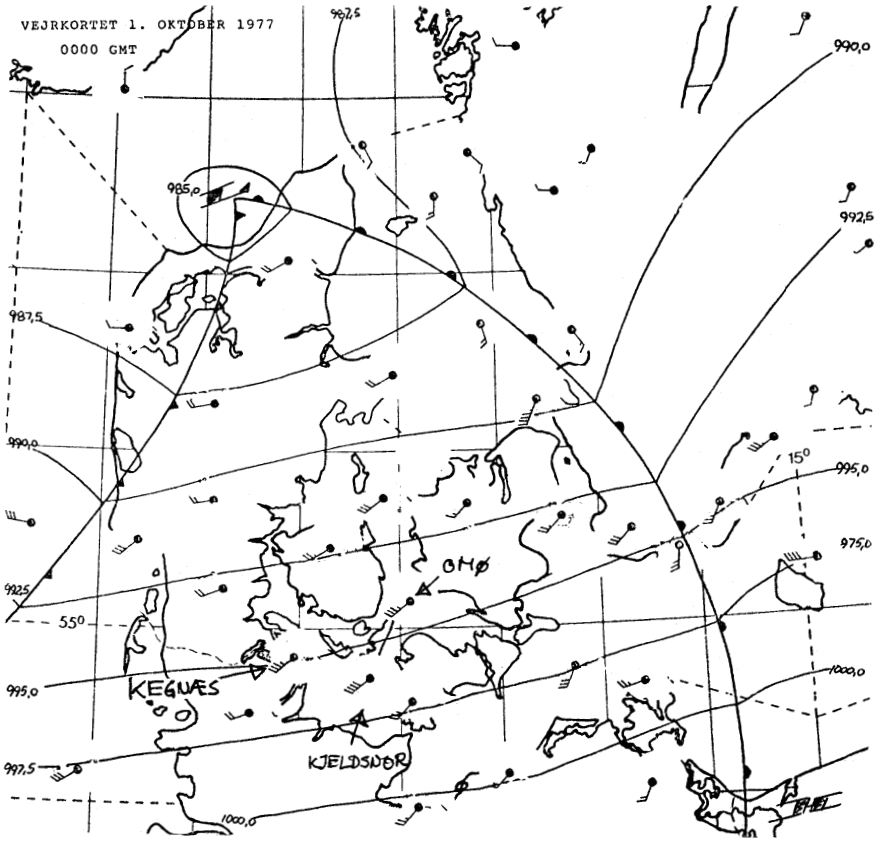

Figure 1.10: Weather map over Denmark, date: 01.10.77, time: 01 am

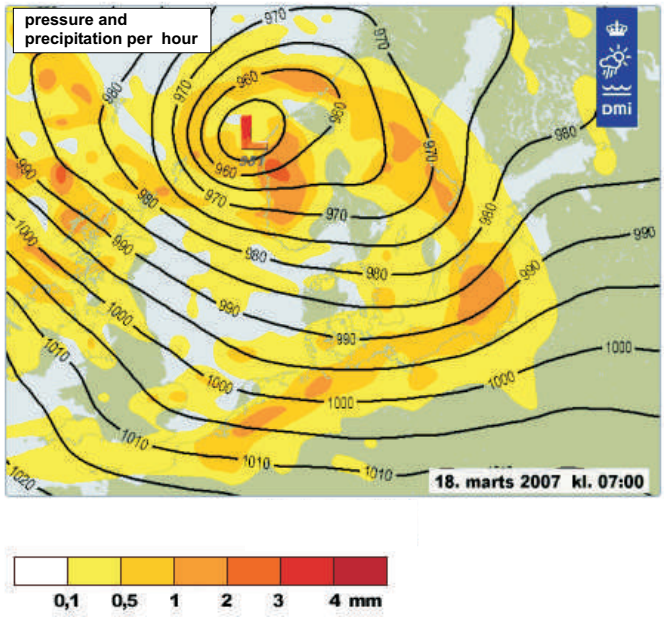

Figure 1.11: Pressure and precipitation forecast for Northern Europe

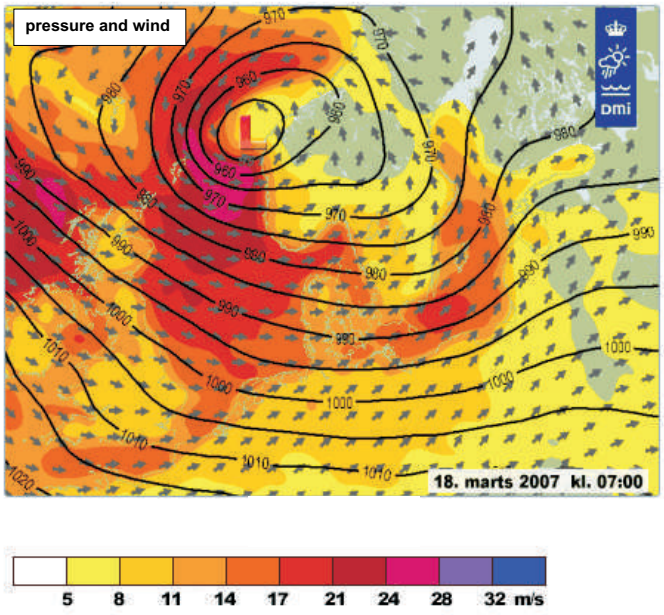

Figure 1.12: Pressure and wind forecast for Northern Europe

It is a bit surprising, but it is clearly seen on weather maps showing both isobars and observed wind directions. Normally the wind direction at a point is shown by a bar pointing in the *opposite* direction of the wind velocity. The strength of the wind is marked by flags on the bar. One whole flag is equivalent to 10 knots = 5 m/s, and half a flag is equivalent to 5 knots = 2.5 m/s. Figure 1.10 is an example of such a weather map, and it shows pressures and winds over Denmark at the first of october 1977 at 01 am.

Notice also that the largest wind velocities occur, where the isobars are closest to each other. The reason for this is explained in the next section.

Today observations and forecasts of weather maps may be downloaded from many web-sites. In Figure 1.12 are shown a wind forecast from Danish Meteorological Institute. Notice that on this map the wind directions are shown with arrows pointing *in* the direction of the wind and the strength is indicated by a color.

1.5 Geostrophic wind

In a storm situation it is natural to divide the flow into a boundary layer close to the ground and a potential flow above this layer. Inside the boundary layer we have substantial shear forces, but the shear forces are so small in the potential flow that we shall neglect them.

The thickness of the boundary layer depends mainly on the roughness of the ground and the wind velocity outside the boundary layer, see section 1.6.

Air behaves like an incompressible newtonian fluid at velocities up to at least 100 m/s, so the ordinary methods from fluid dynamics are applicable to set up equations of motion for an air particle in the atmosphere.

The horizontal external forces on an air particle are a pressure force, $\vec{F}_P$, Coriolis' force, $\vec{F}_{C,h}$ and a shear force $\vec{F}_T$.

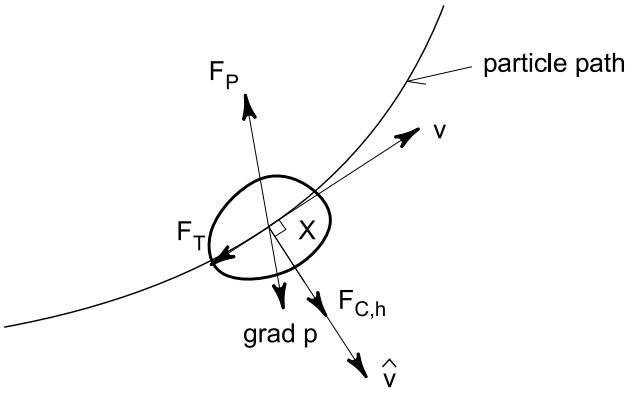

Figure 1.13: External forces acting on an air particle

The pressure gradient, $\operatorname{grad} p$, varies very slowly (the scale is normally many kilometers) and consequently it is a good approximation to consider the gradient constant within the volume,X, occupied by the particle. It is then easy to find the pressure force, $\vec{F}_P$, by means of the so called *gradient-theorem*:

$$\vec{F}_P = \int_A -p\, d\vec{A} = \int_X (-\operatorname{grad} p)\, dX = -\operatorname{grad} p \cdot X \tag{1.8}$$

where A is the surface of the particle, and $d\vec{A}$ is the outward normal to the surface. Coriolis' force is calculated by means of equation (1.7). The shear force is directed against the direction of motion, and in principle it may be expressed as:

$$\vec{F}_T = f(v)\,(-\vec{v}) \tag{1.9}$$

Normally the analytical expression for $f(v)$ is not known, but in practice shear forces are small compared to pressure forces.

The orientation of the forces is sketched in figure 1.13. With these external forces Newton's 2nd law reads:

$$\begin{aligned} m\,\frac{d\vec{v}}{dt} &= \sum \vec{F}_{external} \\ \Leftrightarrow \quad \rho\, X\,\frac{d\vec{v}}{dt} &= \vec{F}_P + \vec{F}_{C,h} + \vec{F}_T \\ \Leftrightarrow \quad \rho\, X\,\frac{d\vec{v}}{dt} &= -\operatorname{grad} p \cdot X + \rho\, X\, f_C\, \hat{v} - f(v)\,\vec{v} \end{aligned}$$

After division by X the equation of motion reads:

$$\boxed{\rho\,\frac{d\vec{v}}{dt} = -\operatorname{grad} p + \rho\, f_C\, \hat{v} - \frac{f(v)}{X}\,\vec{v}} \tag{1.10}$$

Due to very slow variation in time of the pressure field, the speed, v, of a particle rather quickly becomes constant. There might be an acceleration, but it is normal to the velocity. The acceleration vector is easy to find, if the particle path is approximated to a circle with radius R equal to the local radius of curvature.

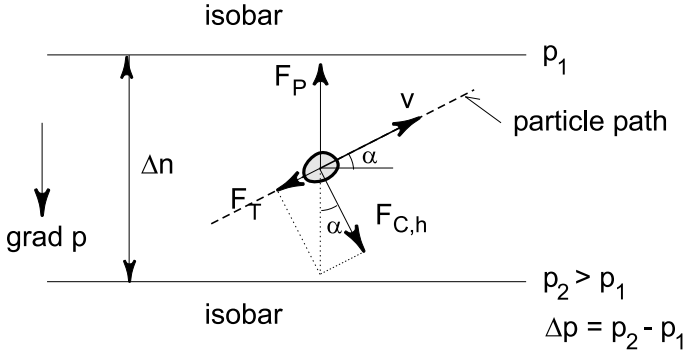

Figure 1.14: External forces acting on an air particle with a straight particle path ($R = \infty$)

In many cases the particle path is nearly straight, and in that situation no acceleration is present i.e. $d\vec{v}/dt = \vec{0}$. See Figure 1.14. In such a case the equation of motion reads:

$$\vec{0} = -\operatorname{grad} p + \rho\, f_C\, \hat{v} - \frac{f(v)}{X}\,\vec{v} \tag{1.11}$$

Due to the presence of the shear force, $\vec{F}_T$, fulfillment of force equilibrium requires that $\vec{v}$ forms the angle α with the isobars, because $\operatorname{grad} p$ is perpendicular to the isobars. The angle is variable, and from Figure 1.14 is seen that the angle is increasing, when the shear force is increasing. Therefore we see the greatest angles near the ground, but normally $\alpha_o < 25^o$, where α_o denotes the angle near the ground.

Outside the boundary layer no shear forces are present, i.e. $\vec{F}_T = \vec{0}$. Here force equilibrium is reached, if Coriolis' force and the pressure force are equal and acting in opposite directions. As the pressure force is perpendicular to the isobars, also Coriolis' force must be perpendicular to the isobars. Therefore the velocity must be parallel to the isobars. The equation of motion reads:

$$\operatorname{grad} p = \rho \, f_C \, \hat{v} \tag{1.12}$$

yielding:

$$|\operatorname{grad} p| = \rho \, f_C \, v \tag{1.13}$$

In case of straight isobars the wind velocity outside the boundary layer is named *geostrophic wind velocity* and denoted U_G.

The pressure gradient is assessed by

$$|\operatorname{grad} p| = \left| \frac{\partial p}{\partial n} \right| \approx \left| \frac{\Delta p}{\Delta n} \right| \tag{1.14}$$

where $\vec{n}$ is perpendicular to the isobars and Δn is the distance between these.

Substitution of these expressions into equation (1.13), yields:

$$\boxed{U_G = |\operatorname{grad} p| \, \frac{1}{\rho \, f_C} \approx \left| \frac{\Delta p}{\Delta n} \right| \, \frac{1}{\rho \, 2 \, \omega \, \sin \lambda}} \tag{1.15}$$

If the radius of curvature of the isobars (and the particle trajectories) is less than 500-1000 km, it is necessary to include the centripetal acceleration in equation (1.10). The wind velocity from such a calculation is named *the gradient wind velocity.*

1.6 Wind in the boundary layer near the ground

In the following only *storm conditions* are considered. This means that the air mass is *fully mixed*, i.e. no differences in density exists and no stratification between cold and hot air is present. As mentioned in the previous section, the air flow can be divided into a boundary layer flow close to the ground and a potential flow outside the boundary layer. The geostrophic velocity, U_G, outside the boundary layer is driving the flow in the boundary layer.

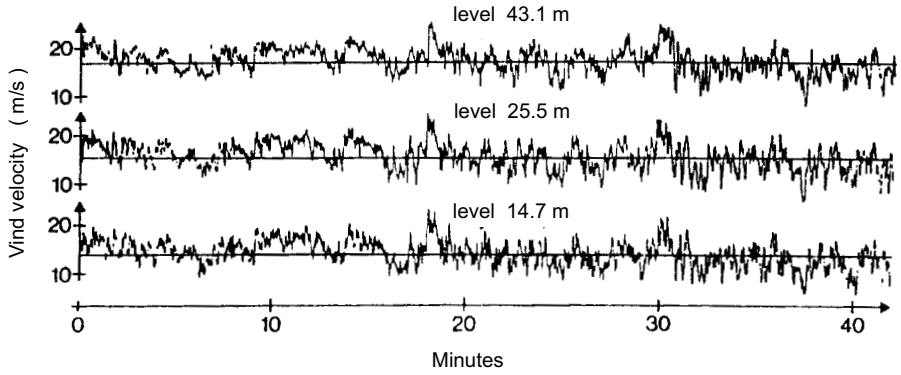

Figure 1.15: Wind velocities measured at Stigsnæs at three differents levels (Dyrbye og Hansen, 1989)

Based on measurements the following is known about the flow in the boundary layer:

- The flow in the boundary layer is strongly turbulent, and the turbulence is created by the passage of the air over the rough surface of the ground. If we denote instantaneous values, v, time averaged values, U, and fluctuations, u, we have:

$$v(z,t) = U(z) + u(z,t) \tag{1.16}$$

$$U(z) = \frac{1}{T}\int_0^T v(z,t)\,dt \tag{1.17}$$

  If nothing else is stated $T = 10$ minutes is applied.

- In practice the values of U also vary in time, but normally very slowly. On the other hand U is strongly dependent of the level, z.

- The standard deviation, σ_u, of time series of the fluctuations $u(z,t)$ is nearly independent of z in the lower part of the boundary layer.

- Short-period variations of $u(z,t)$ do *not* appear simultaneously along a vertical.

- Long-period variations of $u(z,t)$ do appear nearly simultaneously along a vertical.

1.6.1 Wind profile

Measurements of natural wind profiles shows that close to the ground the wind profile approaches that of an ordinary boundary layer over a rough surface. If τ_o denotes the shear stress between the air and the ground, and the so called *friction velocity*, U_F, is defined as:

$$U_F = \sqrt{\frac{\tau_o}{\rho}} \tag{1.18}$$

the expression for the velocity profile reads:

$$U(z) = \frac{1}{\kappa} U_F \ln \frac{z}{z_o} = 2.45\, U_F \ln \frac{z}{z_o} \tag{1.19}$$

Here $\kappa = 0.4$ is named Kármáns' coefficient, z is the distance from the ground and z_o is the roughness length characterizing the size and spacing of the roughness elements on the ground. See Figure 1.16.

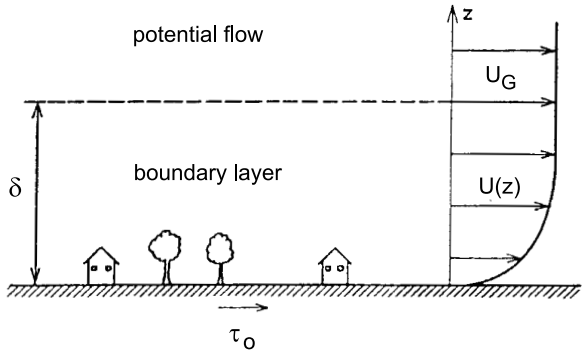

Figure 1.16: Sketch of wind velocity profile

The roughness length for a given surface is assessed from measured values of $U(z)$. $U(z)$ is plotted against $\ln z$, and equation (1.19) is fitted to the data. Because $U(z) = 0$ for $z = z_o$, the z_o-value is found from the intersection between the fitted straight line and the z-axis. Subsequently U_F is calculated by equation (1.19), where known values z_o and $(z, U(z))$ are substituted.

Normally the log-profile, equation (1.19), is valid for $z < 50$ m. For $50 < z < 300$ m a modified log-profile can be used, see e.g. Dyrbye and Hansen (1989).

Characteristic values of z_o are shown in Table 1.1. Normally it can be assumed that $z_o \simeq k_N/30$, where k_N is the Nikuradse grain roughness known from flow in pipes.

Comparison of measured values of U_F and σ_u yields typically:

$$\boxed{\sigma_u \approx 2.5 \cdot U_F} \tag{1.20}$$

where σ_u is the standard deviation of the fluctuations.
The *intensity of turbulence*, $I_u(z)$, is defined as

$$I_u(z) = \frac{\sigma_u}{U(z)} \tag{1.21}$$

and substitution of the equations (1.20) and (1.19) into this expression yields:

$$I_u(z) = \frac{\sigma_u}{U(z)} = \frac{2.5 \cdot U_F}{2.45\, U_F\, \ln \frac{z}{z_o}} = \frac{2.5}{2.45\, \ln \frac{z}{z_o}}$$

or

$$\boxed{I_u(z) \approx \frac{1}{\ln \frac{z}{z_o}}} \tag{1.22}$$

The velocity profile is determined, when U_F is known. From historic weather maps long time series of U_G at many places can be calculated, and to utilize this information we need a relation between U_F and U_G. Davenport (1977) showed that U_F and U_G are related through the expression:

$$U_F \approx U_G \cdot 0.16 \left(\frac{U_G}{f_C\, z_o} \right)^{-0.09} \tag{1.23}$$

where f_C is Coriolis' parameter. Substitution of this expression into equation (1.19) yields:

$$\boxed{U(z) = 2.45\, U_G \cdot 0.16 \left(\frac{U_G}{f_C\, z_o} \right)^{-0.09} \cdot \ln \frac{z}{z_o}} \tag{1.24}$$

In this way $U(z)$ can be determined on basis of values of U_G and z_o.

In Figure 1.17 are shown velocity profiles corresponding to a storm occurring in average every 50 year. The corresponding value of the geostrophic velocity, U_G, is the same for all profiles, but it is clearly seen that the roughness of the ground has great influence on the profiles.

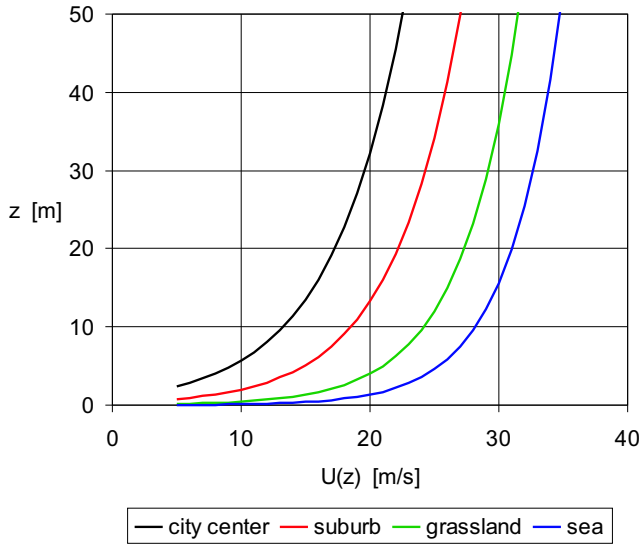

Figure 1.17: Velocity profiles in 50 year storm

terrain	z_o (m)	β (-)	z_G (m)
rough sea	0.005 - 0.010	0.12	250
open grass land	0.010 - 0.10	0.16	300
forest / suburban area	0.30 - 1.00	0.28	400
center of large city	1.00 - 5.00	0.40	500

Table 1.1: *Typical values of the roughness length*

According to Simiu (1978) og Davenport (1977) the thickness of the boundary layer, δ, can be assessed by:

$$\boxed{\delta \approx 0.3 \cdot \frac{U_F}{f_C}} \tag{1.25}$$

Often the velocity profile is approximated by this power-expression:

$$\frac{U(z)}{U_G} = \left(\frac{z}{z_G}\right)^{\beta} \tag{1.26}$$

where the parameters β and z_G are determined by fitting the power-expression to the logarithmic profile. Normally we find $z_G \approx \delta/10$. At this height $U(z) \approx 0.90 \cdot U_G$, and the flow is nearly free of turbulence. In Table 1.1 are shown characteristic values of β and z_G.

Because the boundary layer is very thin compared to the horizontal scale of the flow, the approximations from ordinary boundary theory are applicable. In particular we

use that the pressure field within the boundary layer is determined by the pressure field outside the layer, or, to be more specific, we use it the other way round. Pressure gradients outside the boundary layer are assessed by the pressures measured at the ground (weather maps).

The presence of the shear force on an air particle in the boundary layer is the reason to the observed angle between $\vec{v}$ and the isobars, see Figure 1.14. As the shear force increases towards the ground, $\vec{v}$ is turned more and more counter clock-wise. Measurements show that the expression for α_o, defined as the angle between U_G and $U(10m)$, reads:

$$\sin \alpha_o = 1.7 \cdot \left(\frac{U_G}{f_C \, z_o} \right)^{-0.09} \tag{1.27}$$

For $U_G = 30$ m/s is found:

$$\alpha_o = \begin{cases} 25^\circ \text{ over land} & (z_o = 0.050 \text{ m}) \\ 20^\circ \text{ over water} & (z_o = 0.005 \text{ m}) \end{cases} \tag{1.28}$$

1.6.2 Wind spectrum

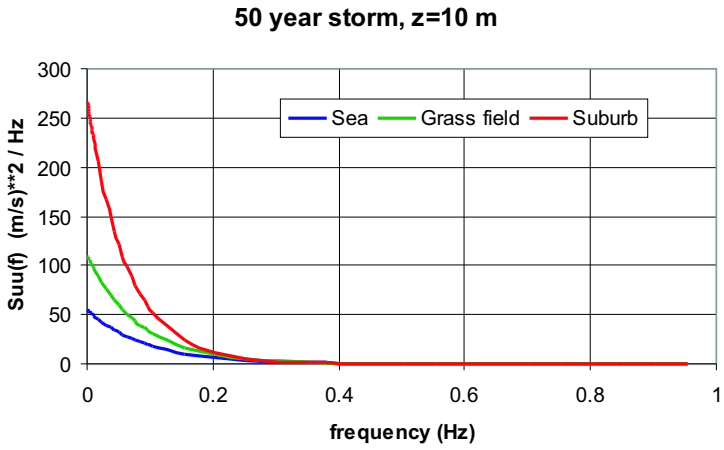

Figure 1.18: Variance spectrum of wind velocity. Linear plot.

The fluctuation $u(t)$ of the wind velocity may be considered a stochastic variable. It has earlier been shown that the standard deviation, σ_u, and therefore also the variance , σ_u^2, depends on terrain roughness and the friction velocity.

The following describes how the variance of $u(t)$ depends on the frequency, f, of the fluctuations. A graph showing this dependence is named a *variance spectrum*.

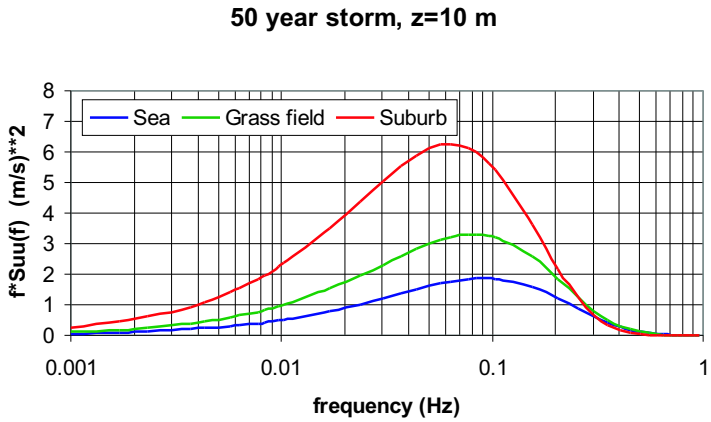

Figure 1.19: Variance spectrum of wind velocity. Logarithmic plot.

The variance spectrum is here denoted $S_{uu}(f)$. The relation between the variance spectrum (sometimes also named auto spectrum) and the variance are per definition:

$$\sigma_u^2 = \int_0^\infty S_{uu}(f)\, df \tag{1.29}$$

and because $\sigma_u \approx 2.5\, U_F$ in the lower part of the boundary layer, the area under the variance spectrum varies only negligible with z.

Typical results from Fourier analysis of a $u(t)$ time series are seen in Fig. 1.18. From these spectra it is seen that substantial part of the variance is located at low frequencies. We also apply variance spectra to describe irregular water waves, but only negligible part of their variance is located at low frequencies.

In order to get a better description of the variance distribution at low frequencies, we use the identity:

$$\int_{f_1}^{f_2} S_{uu}(f)\, df = \int_{f_1}^{f_2} f\, S_{uu}(f)\, d(\ln f) \tag{1.30}$$

A plot of $f\, S_{uu}$ against $\ln f$ therefore improves the resolution at the low frequencies, but the variance is still the area under the curve. See Fig. 1.19.

From theoretical considerations and measurements it is found that variance spectra for wind reads:

$$\boxed{\frac{f\, S_{uu}(z,f)}{\sigma_u^2} = 6.8 \cdot \frac{f\, L(z)}{U(z)} \cdot \left(1 + 10.2 \cdot \frac{f\, L(z)}{U(z)}\right)^{-5/3}} \tag{1.31}$$

where $L(z)$ is a length scale, which according to DS 410 is given by:

$$L(z) = \begin{cases} 100 \left(\frac{z}{10}\right)^{0.3} & \text{hvis } z > z_{min} \\ \\ L(z_{min}) & \text{hvis } z \leq z_{min} \end{cases} \tag{1.32}$$

Values of z_{min} are given in Table 1.2.

1.6.3 Distribution of geostrophic wind, U_G

The wind conditions near the ground are governed by the geostrophic wind, U_G, which can be found on basis of weather maps. The probability distribution of U_G at a given place can therefore be determined by analysis of weather maps covering a longer period. This method was applied in "Vindatlas for Danmark" (1980). The agreement with available distributions based on anemometer measurements was excellent. It turned out that the wind speed is following a Weibull-distribution and nearly the same distribution was found in different parts of the country. Based on this parent probability distribution it is possible to find the extreme value distribution for the geostrophic wind speeds, see e.g. Davenport (1977).

In the Danish Building Code DS 409 it is laid down that buildings should be be dimensioned for the 50-year event, which is the event that appears or is exceeded every 50 year.

If we know the 50-year value of the geostrophic wind, U_G^{50}, the corresponding value close to the ground, $U(10)^{50}$, can be determined, see section 1.6.1.

From the extreme value distribution of U_G above Denmark one finds $U_G^{50} \approx 49$ m/s. Notice that this is an average value and over the North Sea and the west coast of Jutland somewhat higher values are observed.

In Table 1.2 is shown the 50-year values of U_G and $U(10)$ for the 4 types of terrain mentioned in DS 410.

terrain	z_o m	${U_F}^{50}$ m/s	$U(10)^{50}$ m/s	k_t -	z_{min} m
sea	0.01	1.7	28	0.17	2
grass land	0.05	1.9	24	0.19	4
suburb	0.3	2.2	19	0.22	6
center of large city	1.0	2.4	13	0.24	8

Table 1.2: *50-year velocities from DS 410*

U_F^{50} is calculated by equation (1.23) and $U(10)^{50}$ is calculated by equation (1.19), i.e.

$$U(z)^{50} = 2.45\, U_F^{50}\, \ln \frac{z}{z_o} \tag{1.33}$$

In Table 1.2 is also found the terrain factor, k_t, applied in DS 410's expression for the 50-year value of $U(10)$, which reads:

$$U(z)^{50} = U(10)^{50}_{z_o=0.05} \cdot k_t \cdot \ln \frac{z}{z_o} \tag{1.34}$$

In DS 410 the velocity $U(10)^{50}_{z_o=0.05}$ is named the *basic wind velocity*. Comparison of equation (1.33) and (1.34) and substitution of equation (1.20) yields:

$$k_t = \frac{2.45\, U_F^{50}}{U(10)^{50}_{z_o=0.05}} \approx \frac{\sigma_u^{50}}{U(10)^{50}_{z_o=0.05}} = I_u(10)^{50}_{z_o=0.05} \tag{1.35}$$

The terrain factor is therefore the same as the intensity of the turbulence, but this is not mentioned in DS 410! It is also seen that the expression for the standard deviation of the fluctuations reads:

$$\boxed{\sigma_u^{50} \approx k_t \cdot U(10)^{50}_{z_o=0.05}} \tag{1.36}$$

1.6.4 Distribution of wind velocity, $v(z,t)$

Having determined the 50-year event of geostrophic wind and the 10 min. wind at 10 meters height, $U(10)^{50}$, the next issue is to assess the expected maximum value of the wind velocity $v(z,t) = U(z) + u(z,t)$ averaged over another time interval. Such a value is denoted $E(v(z)^{50}_{max})$, and the value depends in the length of the time interval, in which $v(t)$ is observed and averaged over.

From measurements it is known that the fluctuations $u(t)$ follow a normal distribution closely. For a normal distribution the expression for the expectation of max-values, see e.g. Dyrbye and Hansen (1989), reads:

$$E(v(z)^{50}_{max}) = U(z)^{50} + k_p \cdot \sigma_u^{50} \tag{1.37}$$

where the *peak-factor* k_p is:

$$k_p = \sqrt{2\, \ln(T_{obs} \cdot f_{02})} + \frac{0.577}{\sqrt{2\, \ln(T_{obs} \cdot f_{02})}} \tag{1.38}$$

and f_{02} is the frequency for zero-upcrossings of of $u(z,t)$. Just like in wave hydraulics the expression for this variable reads:

$$f_{02} = \sqrt{\frac{m_2}{m_0}} \tag{1.39}$$

where m_0 og m_2 are moments of the variance spectra defined by

$$m_n = \int_0^\infty f^n \cdot S_{uu}(f)\, df \tag{1.40}$$

average time	1 hour	10 min	1 min	15 sec	5 sec	3 sec
conversion factor	0.94	1.00	1.11	1.19	1.24	1.25

Table 1.3: *Conversion factors between 50-year values of velocities at 10 m's height averaged over different time periods,* $z_o = 0.01$ *m.*

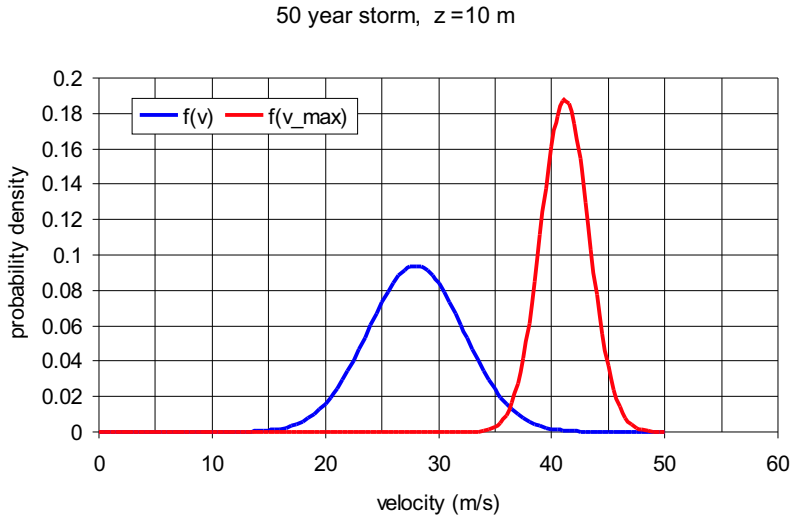

Figure 1.20: Probability density function for v at sea, $z_o = 0.01$ m, and an approximate (see the text) density function for v_{max} corresponding to $T_{obs} = 10$ minutes.

In Fig. 1.20 are shown the probability density function for u and an approximation to the density function for v_{max} corresponding to $T_{obs} = 10$ minutes. The density function for v_{max} has here been approximated by a normal distribution with $E(v_{max}) = 41$ m/s and $\sigma_{v_{max}} \approx \sigma_u/2$.

Normally we find $f_{02} \approx 0.1$ Hz for wind. If the average time is $T_{obs} = 10$ minutes, the expression for k_p reads:

$$k_p = \sqrt{2\,\ln(600 \cdot 0.1)} + \frac{0.577}{\sqrt{2\,\ln(600 \cdot 0.1)}} \approx 3.1 \tag{1.41}$$

If the terrain type is sea, or $z_o = 0.01$ m, the expectation of $E(v(10)^{50}_{max})$ reads:

$$\begin{aligned} E(v(10)^{50}_{max}) &= U(10)^{50} + 3.1 \cdot \sigma_u^{50} \\ &= U(10)^{50} + 3.1 \cdot (2.5\, U_F^{50}) \\ &= 28 + 3.1 \cdot 2.5 \cdot 1.7 = 41 \text{ m/s} \end{aligned} \tag{1.42}$$

Averaging over a time interval always results in an average value lower than the maximum value as can be seen from Table 1.3 showing 50-year values corresponding

to different averaging intervals. Table 1.3 is published in DS 449 dealing with loads on off shore structures. In principle this table is valid for $z_o = 0.01$ m only, but is probably usable for values of z_o also.

The base is $U(10)^{50}$, i.e. the 50-year value of the velocity at 10 m's height averaged over 10 minutes. Normally the velocity averaged over 3 seconds is named the short-time average. It is seen that the ratio between the expectation of v_{max} and the short-time average is $41/(28 \cdot 1.25) = 41/35 = 1.17$.

Chapter 2

Wind loading

2.1 Introduction

In the assessment of the effect of wind loading on a structure, it is very important to distinguish between stiff and flexible structures.

Normally it is simple to calculate the wind loading on a stiff structure and complicated to calculate the effect of wind loading on a flexible structure.

In both cases it should be noticed that peak velocities corresponding to very high frequent fluctuations do not appear simultaneous over large areas. This is due to the fact that high frequent fluctuations corresponds to small eddies. Normally the dimensioning wind load is therefore overestimated, if the wind load is based on $E(v_{max})$ over the entire construction.

2.2 Static wind load

If the construction is very stiff, it is allowable to assume the wind load to be static. The wind load, F, on the area, A, is calculated as

$$F = c \cdot \frac{1}{2} \rho \, v(z_r)^2 \, A \tag{2.1}$$

where c is a shape factor (mainly depending on the shape of the structure), ρ is the density of the air, z_r is a reference height, which for small structures is chosen to be the height of the construction.

By defining the velocity pressure, q, as:

$$q(z) = \frac{1}{2} \rho \, v(z)^2 \tag{2.2}$$

the expression for wind load reads:

$$F = c \cdot q(z_r)\, A \tag{2.3}$$

In order to derive the expression for the maximum velocity pressure stated by DS410, the maximum value of the fluctuations, $u_{max} = k_p \cdot \sigma_u$, is substituted into the expression for the velocity pressure. This yields:

$$\begin{aligned}
q_{max}(z) &= \frac{1}{2}\rho\,(U(z) + u_{max})^2 \\
&= \frac{1}{2}\rho\,(U(z)^2 + 2U(z)\,u_{max} + u_{max}^2) \\
&\approx \frac{1}{2}\rho\,(U(z)^2 + 2U(z)\,u_{max}) \\
&= \frac{1}{2}\rho\,(U(z)^2 + 2U(z)\,k_p \cdot \sigma_u) \\
&= \frac{1}{2}\rho\,U(z)^2\left(1 + 2\,k_p \frac{\sigma_u}{U(z)}\right) \\
&= \frac{1}{2}\rho\,U(z)^2\,(1 + 2\,k_p\,I_u(z))
\end{aligned} \tag{2.4}$$

Here the definition of turbulence intensity has been applied, and it has been assumed that $u_{max}^2 \ll U(z)^2$. This assumption reduces the velocity pressure approximately 6 %. Normally it is unwise to reduce a driving load, but here it is justified by the fact that u_{max} do not occur simultaneously over the entire structure.

For the 50-year event equation (2.4) yields (as stated in DS410) :

$$q_{max}(z)^{50} = \frac{1}{2}\rho\,(U(z)^{50})^2(1 + 2\,k_p I_u(z)) \tag{2.5}$$

2.3 Dynamic wind load

For a flexible structure it is necessary to consider the wind load as a dynamic load in order to capture possible resonance problems. Notice that important dynamic loads can exist in both the flow direction and perpendicular to that. However, the present notes treats only the dynamic loads in the flow direction.

Often Morison's equation is chosen as the load model, and for slender structures the inertial force can be neglected. In that case the extended Morison's equation reads:

$$F(t) = c_D \cdot \frac{1}{2} \rho \left(v(t) - \dot{x} \right)^2 A \tag{2.6}$$

where
$F(t)$ is the wind load acting on the area, A
x is the displacement of the construction
$\dot{x}$ is the velocity of the construction
c_D is a form factor
ρ is the density of the air.

The most straightforward dynamic model for a slender konstruction is sketched in Figure 2.1.

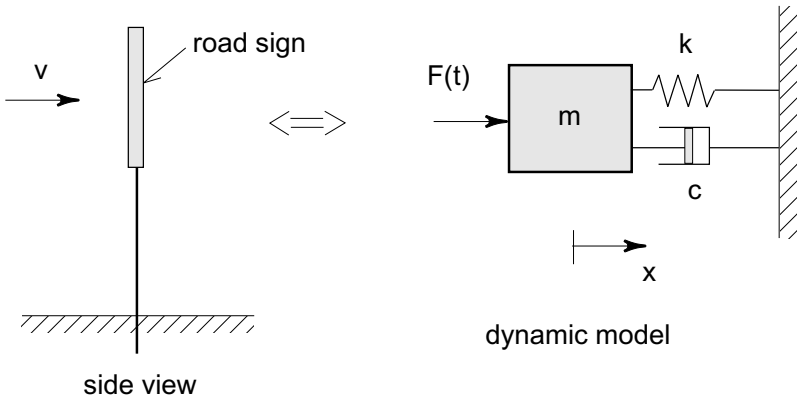

Figure 2.1: Dynamic model of a road sign, 1 degree of freedom (1 DOF)

Newton's 2. law for this system reads:

$$m\,\ddot{x} = \sum F_{external} = -k\,x - c\,\dot{x} + F(t) \tag{2.7}$$

where x is displacement, k is the stiffness, and c is the damping constant. This equation is rewritten to:

$$m\,\ddot{x} + c\,\dot{x} + k\,x = F(t) \tag{2.8}$$

The expression for the wind force, $F(t)$, is rewritten by substitution of $v(t) = U+u(t)$ yielding:

$$\begin{aligned} F(t) &= c_D \frac{1}{2} \rho [v - \dot{x}]^2 A \\ &= c_D \frac{1}{2} \rho [v^2 + \dot{x}^2 - 2\, v\, \dot{x}] A \\ &= c_D \frac{1}{2} \rho \left[(U+u)^2 + \dot{x}^2 - 2(U+u)\, \dot{x} \right] A \\ &\approx c_D \frac{1}{2} \rho \left(U^2 + 2\, U\, u - 2\, U\, \dot{x} \right) A \\ &= c_D\, A \frac{1}{2} \rho U^2 + c_D\, A\, \rho\, U\, u - c_D\, A\, \rho\, U\, \dot{x} \\ &= \overline{F} + c_D\, A\, \rho\, U\, u - c_D\, A\, \rho\, U\, \dot{x} \end{aligned} \tag{2.9}$$

where $\overline{F} = c_D\, A\, \frac{1}{2}\, \rho\, U^2$ is the 10 minutes average of the wind load. Substitution of equation (2.9) into equation (2.8) gives:

$$m\, \ddot{x} + c\, \dot{x} + k\, x = \overline{F} + c_D\, A\, \rho\, U\, u(t) - c_D\, A\, \rho\, U\, \dot{x} \tag{2.10}$$

Notice that a term is proportional to $\dot{x}$ in the dynamic part of the load. If this term is moved to the left-hand side of the equation, it may formally be considered as a damping term, as equation (2.8) now reads:

$$m\, \ddot{x} + \left(c + c_D\, A\, \rho\, U \right) \dot{x} + k\, x = \overline{F} + c_D\, A\, \rho\, U\, u(t) \tag{2.11}$$

The extra damping term in equation 2.11 is named *aerodynamic damping* due to the dependence of U. In practice it is a very important term, because an increase in the damping gives a reduction of the motions (and thereby in the strains and stresses in the construction).

Time averaging of all terms of equation (2.11) gives:

$$k\, \overline{x} = \overline{F} \tag{2.12}$$

as $\overline{u} = 0$, and one necessarily must have $\overline{\ddot{x}} = \overline{\dot{x}} = 0$. Otherwise the road sign would move to another place! Consequently the road sign is oscillating around the average position $\overline{x}$.

The easiest course is taken if we define y as the deviation in displacement from the average position, i.e.

$$x = \overline{x} + y \tag{2.13}$$

and denote the dynamic part of the load $F_y(t)$, i.e.

$$F_y(t) = c_D\, A\, \rho\, U\, u(t) \tag{2.14}$$

Substitution of these expressions into equation (2.11) gives:

$$m\,\ddot{y} + \Big(c + c_D\,A\,\rho\,U\Big)\,\dot{y} + k\,y = F_y(t) \tag{2.15}$$

Due to the linear relation between $u(t)$ and $F_y(t)$, it is known that

$$\sigma_F = c_D\,A\,\rho\,U \cdot \sigma_u \tag{2.16}$$

and that the expression for the variance spectrum for F_y reads:

$$S_{FF}(f) = (c_D\,A\,\rho\,U)^2 \cdot S_{uu}(f) \tag{2.17}$$

where the expression for $S_{uu}(f)$ e.g. can be found in DS410. Notice that this simple conversion from wind spectrum to load spectrum is based on the assumption that $u(t)$ has the same value over A, which in general is not true. The velocity fluctuations are caused by eddies, and the highest frequencies corresponds to the smallest eddies. Above a certain frequency the eddies are small compared to A causing the $u(t)$-value to vary over A. The loading of the road sign is therefore overestimated by equation (2.17). In practice this problem is solved by introduction of a reduction factor depending of the frequency, see e.g. Dyrbye og Hansen (1989).

Equation (2.15) is thoroughly discussed in all standard textbooks on vibration theory and below is mentioned a few results.

For a *linear system* a harmonic load

$$F_y(t) = a_F \cdot \sin(2\,\pi\,f\,t) \tag{2.18}$$

causes a harmonic displacement

$$y(t) = a_y \cdot \sin(2\,\pi\,f\,t + \varphi(f)) \tag{2.19}$$

where $f = 1/T$ and $\varphi(f)$ is a phase shift (unimportant here!). The relation between the amplitudes is named the *frequency response*-function for the system. It is normally denoted $|H(f)|$, and from vibration theory is we have:

$$|H(f)|^2 = \left(\frac{a_y(f)}{a_F(f)}\right)^2 = \frac{1}{[k - m(2\,\pi\,f)^2]^2 + [(c + c_D\,A\,\rho\,U)(2\,\pi\,f)]^2} \tag{2.20}$$

As the system is linear, the variance spectrum for the displacement y reads:

$$S_{yy}(f) = |H(f)|^2 \cdot S_{FF}(f) \tag{2.21}$$

Substitution of equation (2.17) into equation (2.21) yields:

$$S_{yy}(f) = |H(f)|^2 \cdot (c_D\,A\,\rho\,U)^2 \cdot S_{uu}(f) \tag{2.22}$$

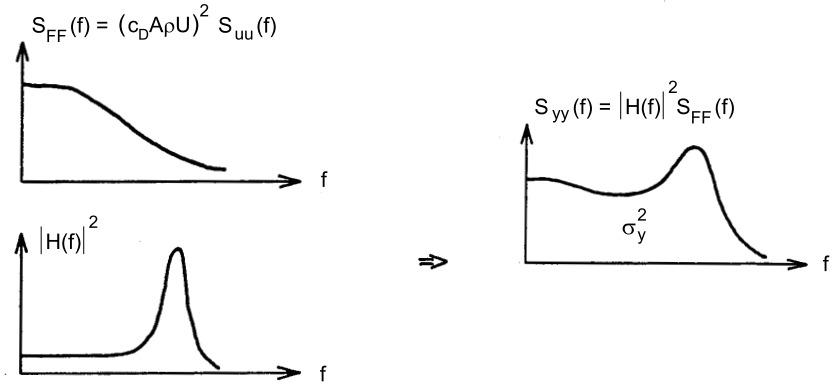

Figure 2.2: Relation between variance spectra for force and displacement

It is seen that the variance spectrum for the displacement from the average position can be calculated directly from the wind spectrum, and the variance, σ_y^2, is equal to the area below $S_{yy}(f)$.

If $y(t)$ is normally distributed, we can assess the maximum displacement y_{max} by

$$y_{max} = k_p \cdot \sigma_y \tag{2.23}$$

where the expression of k_p is given by equation (1.38). In fact $y(t)$ follows a normal distribution, as we know that the normal distribution of $u(t)$ causes normal distribution of $F_y(t)$. It is known also that a linear system loaded by a normally distributed force force has a normally distributed response. Therefore, $y(t)$ is normally distributed.

The peak factor, k_p, depends on the time of observation T_{obs}, the zero-upcrossing frequency f_{02} of the y-time series. See e.g. DS410 how to calculate f_{02} for different types of constructions. DS410 also states that it is on the safe side to assume $k_p = 3.5$ in the assessment of y_{max}.

Finally the expectation of total displacement of the road sign reads:

$$x_{max} = \overline{x} + 3.5 \cdot \sigma_y \tag{2.24}$$

From Figure 2.2 is seen that the size of σ_y depends on the shape of $|H(f)|^2$, and we know that $|H(f)|$ depends on the design of the construction via the variables m, k og c.

Therefore, in practice it is essential to strive for a design, which places the peak of $|H(f)|$ at frequencies, where only small values of $S_{uu}(f)$ (and $S_{FF}(f)$) are present.

References

Davenport, A. G. (1977), *Wind Structure and Wind Climate, Safety of Structures under Dynamic Loading, Vol. 1*, Trondheim.

Simiu, E. and Scanlan, R. H. (1978), *Wind Effects on Structures.*

Petersen, E. L., Troen, I. og Frandsen, S. E. (1980), *Vindatlas for Danmark*, Risø.

DS 449 (1983) , *Pile-supported Offshore Steel Structures*, Teknisk Forlag.

Meriam, J. L. and Kraige, L. G. (1987), *Dynamics, Engineering Mechanics, Vol. 2*, John Wiley and Sons.

Dyrbye, C, og Hansen, S. O. (1989), *Vindlast på bærende konstruktioner*, SBI-anvisning nr. 158, Statens byggeforskningsinstitut.

DS 410 (1998) , *Norm for last på konstruktioner*, Dansk Standard.

ISSN 1901-7286
DCE Lecture Notes No. 12